

# A Detailed Comparison of X-ray and Radio Structure of the Cygnus Loop

D.A. Leahy<sup>1</sup>

<sup>1</sup>Dept. of Physics and Astronomy, University of Calgary, Calgary, Alberta T2N 1N4, Canada

## Abstract

The Cygnus Loop is one of the largest and nearest supernova remnants. It has been mapped by the PSPC detector of the Röntgen-Satellit ROSAT (Aschenbach and Leahy, 1999) resulting in the highest-sensitivity complete x-ray image of this remnant. The radio structure of the Cygnus Loop was observed at 1420 MHz with the synthesis telescope of the Dominion Radio Astrophysical Observatory (Leahy, Roger and Ballantyne, 1997) with similar spatial resolution. Here, is reported on a detailed comparison of the structure of the Cygnus Loop in x-rays and radio.

## 1 Introduction:

The Cygnus Loop is a well-studied large ( $3^\circ$  diameter) supernova remnant (SNR) with a clear shell-type morphology in x-ray, optical, infrared and radio bands. The radio map at 1420 MHz was first presented by Leahy and Roger (1997) in a study of the radio polarization of the Cygnus Loop.

The optical nebulosity is clearly visible on the Palomar sky survey plates. A recent optical and x-ray study of an optical knot on the SE rim of the Cygnus Loop is given by Graham et al. (1995). A review of older x-ray observations of the Cygnus Loop is found in Leahy, Fink & Nousek (1990). An x-ray spectroscopic study of the NE rim of the Cygnus Loop with the ASCA detectors is given by Miyata et al. (1994). Miyata et al. (1998) have detected a metal-rich plasma at the center of the Cygnus Loop with the ASCA detectors, giving evidence that the Cygnus Loop was the result of a type II supernova. The ROSAT PSPC map (Aschenbach and Leahy, 1999, Leahy and Aschenbach, 1996) is the best full x-ray map of the Cygnus Loop.

The comparison of radio and x-ray emission from supernova remnants is of great interest.



Figure 1: The 1420 MHz radio map of the Cygnus Loop, made with data from the Dominion Radio Astrophysical Observatory Synthesis Telescope.

The x-ray emission traces the hot gas behind the shock front, while the radio emission is from the relativistic electron population emitting synchrotron radiation in the ambient magnetic field. The synchrotron emission should have both upstream (relative to the shock position) and downstream components. The extent of these is governed by both the amplification of the magnetic field in the shock compression and the relative density of relativistic electrons upstream and downstream. The latter is determined by the scattering mechanisms for the electrons, which as yet are not well understood (e.g. see the review by Draine and McKee, 1993).

Here, some results of a comparison of the x-ray and radio images of the Cygnus Loop are summarized.

## 2 Images and Analysis

The radio image was made from observations with the Dominion Radio Astrophysical Observatory's Synthesis Telescope at 1420 MHz. The data analysis is described in Leahy, Roger & Ballantyne (1997). This radio image is the highest resolution complete radio image of the Cygnus Loop, and has a resolution of  $\sim 1$  arcminute. Figure 1 shows the radio image in greyscale form.

The x-ray map for the Cygnus Loop was made from the observations of the ROSAT all-sky survey. The ROSAT all-sky survey maps of the Cygnus Loop have been published in Leahy & Aschenbach (1996) and Aschenbach & Leahy (1999). The latter also contains a description of the data analysis. The map that was used for this study was made using the highest possible spatial resolution. To do this, the broad energy band (0.2-2.0 keV) was used and the map was made using only photon events within 20 arcminutes from the center of the optic axis on the PSPC detector. The resulting x-ray map of the Cygnus Loop is shown in Figure 2.

Both the x-ray and radio maps were transformed to the same coordinates and pixel size. The final pixel size for both maps was  $40''$ .

Next a set of slits, each 5 pixels wide by 100 pixels long, were chosen to completely cover the outer shock of the Cygnus Loop, with the long dimension locally perpendicular to the shock. The definition of shock position was taken here as defined by the x-ray map. This was done since the x-ray should be the best indicator of the outer shock. Also the x-ray background is much more



Figure 2: The x-ray map of the Cygnus Loop, made with data from the ROSAT All-Sky Survey.

uniform and of relatively lower level, than the radio background, which meant determination of the outer edge in x-rays was simpler than in radio. A total of 150 slits resulted. A second set of slits was chosen (locally) perpendicular to the long prominent radio filament known as the "Serpent". This second set of slits was defined using the radio image.

Profiles in x-ray and in radio were produced by averaging along the width of each slit.

The x-axes of all of the profiles were shifted so that the outer edge of the x-rays was at  $x=0$ , and flipped if necessary so that the interior of the Cygnus Loop was on the right (for the profiles of the Serpent feature  $x=0$  was defined by the peak of the radio emission). Figure 3 shows a set of 10 aligned profiles from the x-ray image, for the 10 slits along the south east rim of the Cygnus Loop. The rise in x-ray at the position of the shock is clearly seen, as is the decrease of emission interior to the shock.

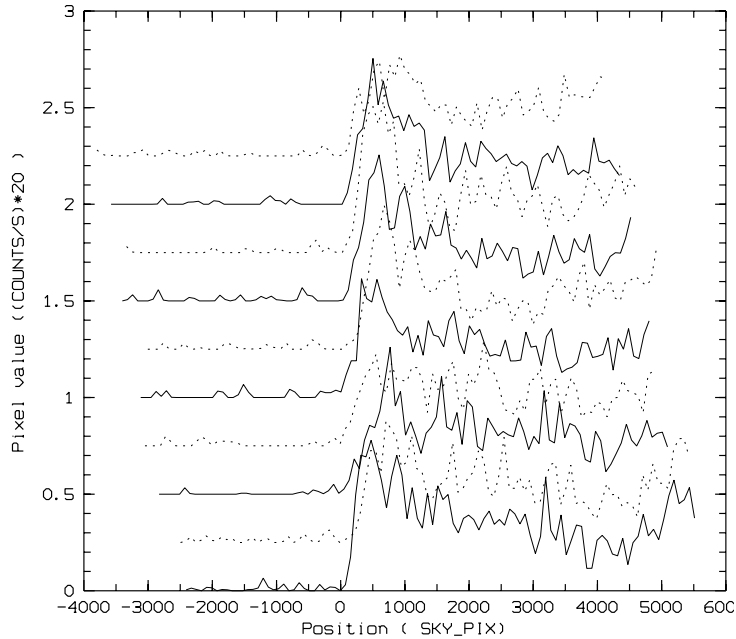


Figure 3: The brightness profiles in xray of the 10 slits along the southeast rim of the Cygnus Loop.

Figure 4 shows the set of 10 profiles (aligned using the x-ray profiles from the radio image), for the same 10 slits along the south east rim.  $x = 0$  marks the position of the shock as determined in x-rays.

As seen from Figures 3 and 4, the variation in the profiles in x-ray is fairly small, but the variation in the profiles in radio is fairly large. Much of the variation in the radio profiles is due to background radio emission, from point sources and extended emission. For all of the profile pairs for the outer shock, the positions of the outer edges, the positions and values and of the peaks of x-ray and radio emission (ignoring point sources), and the levels of exterior (background) and interior emission have been measured. There is considerable variation in these parameters, indicating that the properties of the shock, such as the pre-shock density (which is a major factor in determining the x-ray brightness) and the magnetic field (which is a major factor in determining the shock acceleration efficiency and the radio brightness) vary considerably around the rim of the Cygnus Loop.

The average of all of the profiles for the entire outer shock of the Cygnus Loop was also computed. The profiles were aligned using the rise in x-rays to define the shock position. Despite the wide variation the individual x-ray and radio profiles, the mean profile has a smooth shape. This mean profile shows nearly the same shape in radio and x-rays except that the radio emission has a significant uniform background outside of the shock. This background is not associated with the Cygnus Loop since it extends for as far as measured (several tens of arcminutes) without changing. The shapes of the mean x-ray and radio profiles are as follows: sharp rise from the shock front ( $x = 0$ , defined in x-ray) to a maximum, which occurs over a distance of  $\sim 4$  arcminutes; then a slow decrease towards the center which occurs over a distance scale of  $\sim 30$  arcminutes. The x-ray profile continues to decrease

toward the center, whereas the radio profile inwards of  $\sim 30$  arcminutes from the shock shows an increase towards the center. The observed profile in x-rays is consistent with the simple Sedov model prediction, once one takes into account (somewhat uncertain) projection effects. The mean profile in radio has a small region just outside the shock front, not present in the mean profile in x-rays, which shows weak excess radio emission extending upstream of the shock by  $\sim 3$  arcminutes. More study of this will be needed to verify whether this is related to upstream emission from relativistic electrons accelerated by the shock.

### 3 Discussion

The comparison radio and x-ray images of supernova remnants promises to give a number of interesting physical results. For the

Cygnus Loop, measurement of x-ray and radio profiles at the outer shock shows many cases with radio emission inside of, coincident with, or outside of the x-rays. Due to variance with theory for a simple geometry, the most straightforward explanation is that we are observing emission from different shock structures, with greatly varying thermal particle and relativistic particle densities and magnetic fields, along the line of sight.

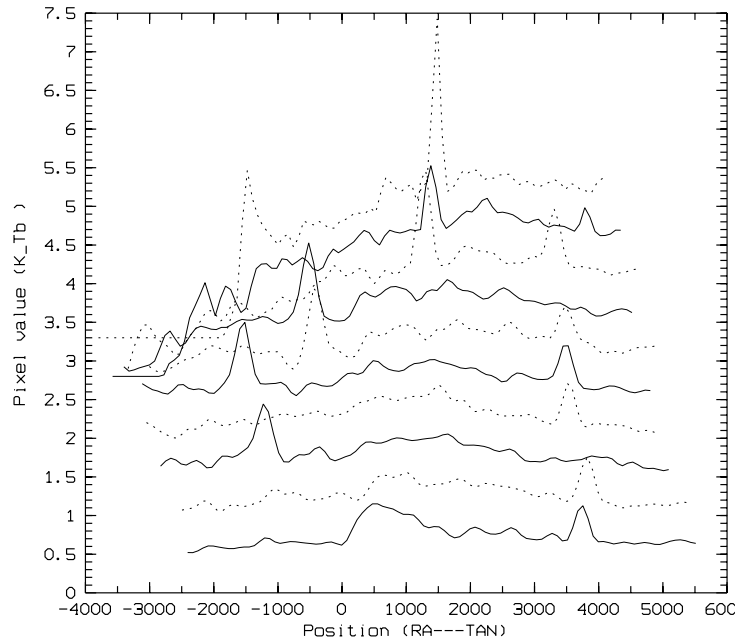


Figure 4: The brightness profiles in radio of the 10 slits along the southeast rim of the Cygnus Loop.

the line of sight. The mean profile for the outer shock shows some evidence for upstream radio emission from relativistic electrons accelerated by the shock. If verified, this would constitute the first detection of the radio emission from upstream relativistic electrons.

### References

- Achterberg, A., Blandford, R. & Reynolds, S. 1994, A&A 281, 220
- Aschenbach, B. & Leahy, D. 1999, A&A 341, 602
- Draine, B. & McKee, C. 1993, ARAA 31, 373
- Graham, J. et al. 1995, ApJ 444, 787
- Leahy, D., Fink, R. & Nousek, J. 1990, ApJ 363, 547
- Leahy, D., Roger, R. & Ballantyne, D. 1997, AJ 114, 2081
- Leahy, D. & Aschenbach, B. 1996, in Proceedings of Roentgenstrahlung from the Universe Wurzburg, MPE Report 263
- Miyata, E. et al. 1994, PASJ 46, L101
- Miyata, E. et al. 1998, PASJ 50, 257